Advances in Remote Sensing, 2024, 13, 73-88
https://www.scirp.org/journal/ars
ISSN Online: 2169-2688
ISSN Print: 2169-267X

Evaluation of Convolutional-Long Short-Term Memory Model in Predicting Surface Displacement of Underground Mines

Saviour Mantey*, **Yao Yevenyo Ziggah**, **Isaac Selasi Kojo Attipoe**

Department of Geomatic Engineering, University of Mines and Technology, Tarkwa, Ghana
Email: *smantey@umat.edu.gh, yyziggah@umat.edu.gh, iskattipoe@gmail.com

How to cite this paper: Mantey, S., Ziggah, Y.Y. and Attipoe, I.S.K. (2024) Evaluation of Convolutional-Long Short-Term Memory Model in Predicting Surface Displacement of Underground Mines. *Advances in Remote Sensing*, **13**, 73-88.
https://doi.org/10.4236/ars.2024.133004

Received: August 2, 2024
Accepted: September 20, 2024
Published: September 23, 2024

Abstract

Surface stability is essential in underground mines health management systems. Unexpected Surface displacement in underground mines could lead to loss of lives, injuries, and economic losses. To reduce or neutralise the adverse effects of surface displacement, it is vital to monitor and accurately predict them and unravel their mechanisms. In recent years, Convolutional Neural Network (CNN) and Long Short-Term Memory (LSTM) have proven effective in predicting complex problems. However, CNN neglects the dynamic dependency of the input in the temporal dimension, which affects surface displacement features. The Convolutional-LSTM model can dynamically learn the temporal dependency among input features via the feedback connections in the LSTM to improve accurate captures of surface displacement features. This study focused on evaluating the C-LSTM model in predicting surface displacement of underground mines and assessed the predictive capabilities and generalisation strength of using hybridised ANN models. Geodetic and geotechnical data gathered from a Gold Mine in Ghana was used. The three models were tested on experimental data collected at Monitoring Scan Point 3. It was observed from the prediction output that all the methods could provide applicable and practical results. However, using indicators like root mean square error (RMSE) and correlation coefficient (R) in assessing the output of the prediction, the C-LSTM had the best prediction output. This study contributes to the advancement of accurate and efficient prediction of surface displacement of underground mines, ultimately enhancing and assisting safety operations.

Keywords

ANN, CNN, LSTM, C-LSTM, Underground Mines, Surface Displacement

1. Introduction

As the availability of greenfield mineral resources diminishes, the practice of reworking established and abandoned surface mines to access remnants and previously unmineable materials may become more frequent. In such instances, underground mining methods may be implemented to gain access to resources that were previously considered too difficult, dangerous, or economically unviable to extract. It is widely recognised that the mining industry plays a crucial role in the global economy, providing essential resources for various sectors [1]. Nevertheless, underground mining operations often give rise to imperative challenges due to the potential for ground movement and associated surface displacement, representing one of the operational risks requiring continuous mitigation. Another critical risk associated with underground mining is ground fall, characterised by the sudden and unexpected collapse of the roof or walls of an underground mine. Ground fall constitutes one of the significant causes of fatalities, injuries, and damage to equipment and infrastructure within underground mines [2]. Due to the phenomena in the Earth's crust, including plate tectonics, groundwater level fluctuations, and landslides, continuous motions are in effect. Displacement, in this context, refers to the apparent changes in the shape of objects or structures both above and below the Earth's surface due to the influence of physical forces resulting from these ongoing movements [3] [4]. Although these changes may be insignificant, they could lead to catastrophic events if displacement trends are left unmonitored. Monitoring their responses to stresses is critical not only for understanding the behaviour of the Earth's surface, but also for taking preventive measures before potential damage occurs [3]. This establishes the field of displacement analysis.

The accurate prediction and monitoring of these displacements are crucial for ensuring the safety of both mining personnel and nearby communities, as well as for preventing costly damage to infrastructure and the environment [5]. Traditional methods for predicting surface displacement in underground mines primarily rely on empirical observations and monitoring activities, which can be costly, time-consuming, and may not always be accurate and effective. In contrast, this research focuses on the utilisation of Artificial Neural Networks (ANNs) to predict surface displacement caused by underground mining activities [6]. ANNs have proven to be highly effective in solving complex problems, including prediction tasks in various fields. By training an ANN model using historical data from underground mining operations and corresponding surface displacements, it becomes possible to create a predictive model capable of estimating the extent of surface displacement based on specific mining parameters and geological features [7]. ANNs are established as computational models that simulate the structure and function of the human brain, allowing them to extract patterns, trends, and relationships from large, complex datasets and make predictions based on historical data. The accuracy and reliability of the developed ANN model is assessed through rigorous validation procedures [8]. This validation entails comparing the predicted surface displacement values generated by the model with actual measurements obtained from monitoring systems in real mining scenarios. A few researchers have explored the use of ANNs for surface displacement prediction in underground mines. Chern *et al.* [9] used a back-propagation neural network model to forecast lateral wall displacement in top-down excavation. Zhang *et al.* [10] used multivariate adaptive regression splines for the determination of Earth Pressure Balance (EPB) tunnel-related maximum surface settlement. However, there are still several challenges that need to be addressed before ANNs can be widely used in the mining industry for this purpose. One of the main challenges pertains to the lack of high-quality data. Surface displacements are rare, and collecting such data is exceptionally difficult [6]. Another challenge revolves around the necessity to develop robust and accurate models that can predict surface displacement events in real time. Displacement analysis encompasses two primarily utilised methods: the Geotechnical Structural Method and the Geodetic Survey Methods. In geotechnical applications, substantial structural component displacements in soil, such as penetrometers or footings, are prevalent, necessitating a proficient large displacement approach to assess the geometric alterations induced by variations in surface profiles and distortions of specific soil layers [11]. On the other hand, Geodetic Survey Methods involve the field of geodesy, which investigates the material composition of the Earth and its gravitational field, studying variations over time and distance.

For displacement analysis, geodetic data are repeatedly collected at various time epochs, with observations at each epoch being independently adjusted. Displacement model parameters are deduced from the alterations in coordinates between these epochs, forming the basis for inferences regarding surface displacement [12]. The prediction of surface displacement events in underground mines is a challenging task that necessitates the development of accurate and robust models. The use of ANNs show promise, but several challenges need to be addressed before ANNs can be widely utilised in the mining industry. Therefore, the evaluation of the performance of the Convolutional-Long Short-Term Memory (C-LSTM) model for predicting surface displacement in underground mines is the primary objective of this research, with a focus on addressing the challenges bewritten above.

2. Materials and Methods

2.1. The Study Area

The study was conducted on the wall formation of an underground mine in Ghana. Mineralised concentration zone along the hanging (high) wall is proven to be of the highest conglomerate band in the Basal reef. The underground mine operations exploit narrow, tabular auriferous conglomerates within the paleo placer deposit of the banket series of the Tarkwaian basin. **Figure 1** shows the map of the study area.

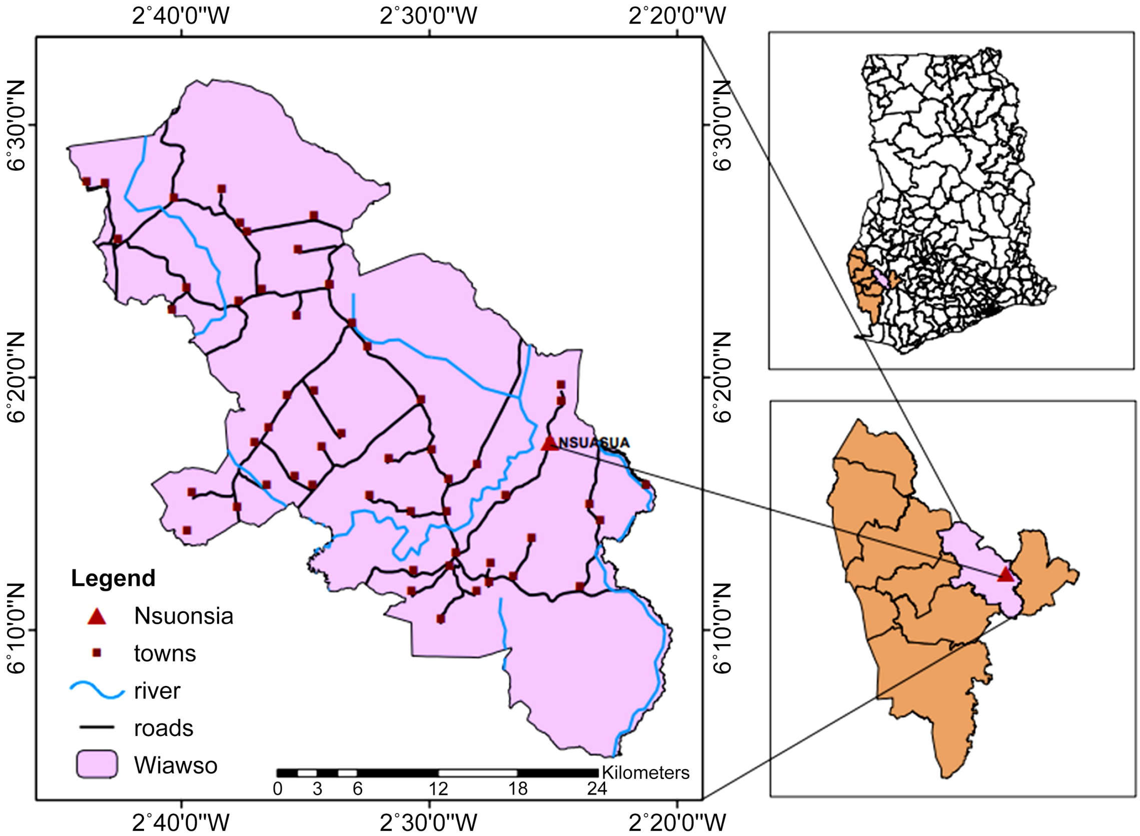

Figure 1. A map of the study area.

2.2. Materials

To be able to assess the predictive efficiency and generalisation strength of combining two distinct artificial intelligence methods for surface displacement analysis, surface displacement data of the underground mine, which has been observed every day for a 1 year and 2 months (423 observations) were used in this research. The underground mine used geodetic and geotechnical surface displacement techniques, taking void scans using drone and other monitoring equipment. The data had variables such as Northings, Eastings, Elevations, Rock Quality Index (Q), Rock Quality Designation (RQD), Peak Particle Velocity, Internal Comprehensive Strength (ICS), Blast Distance, Log of Blast Distance, Density, and Displacement. Monitoring Scan Point 3 (MSP3), is one of the several monitoring points underground, used in this research. As a component of the safety measurement system on the mine, observations are made to acquire certain geodetic and geotechnical variables needed for safety analysis and stability of the mine. Software including python and ArcGIS were used for data processing in this research.

2.3. Methods Used

The methods used in this research comprise of CNN model, LSTM and the hybrid C-LSTM model. The various methodologies employed in this research work is illustrated in Figure 2.

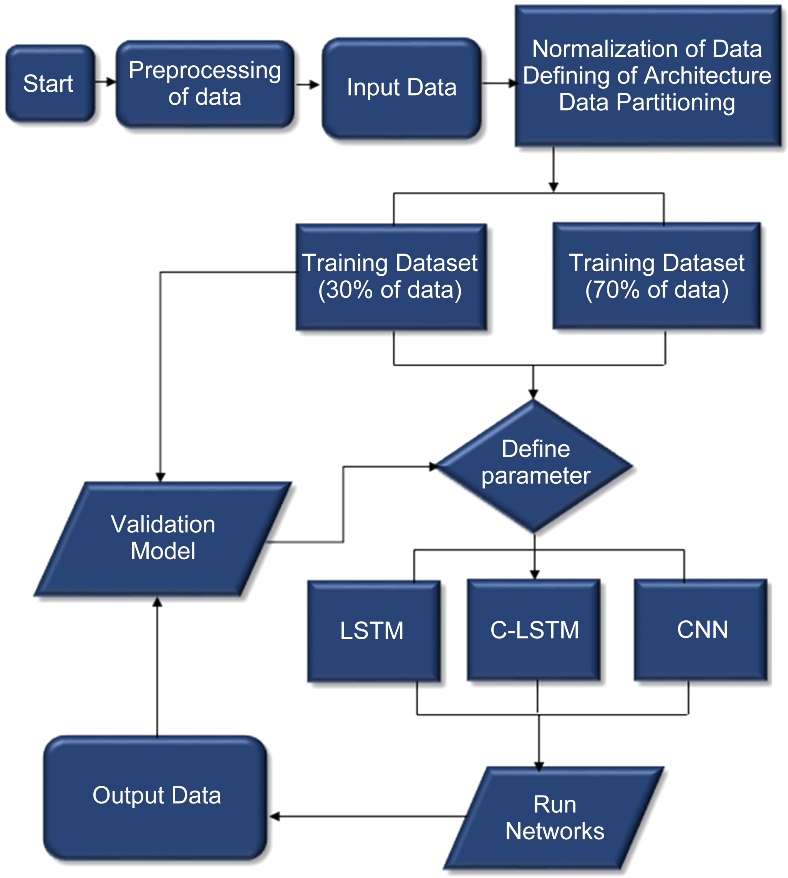

Figure 2. A flowchart of the methods used to develop the models.

2.3.1. Data Preparation

The data is transformed in a format that is recognised by the software being used *i.e.*, python. Descriptive statistical analysis was performed for the individual input parameters, to check for anomalies and bias within the data. As no errors were encountered, the data was divided into two in a ratio of 7:3 as 70% of the data for the training dataset and 30% of the data for the testing dataset. It is to be noted that the testing dataset is partitioned into two *i.e.*, testing and validation data. A correlation coefficient map is produced to analyse the relationship between the various input parameters, as shown in **Figure 3**.

2.3.2. Convolutional Neural Network (CNN)

The CNN is a sort of supervised ANN method used to resolve both linear and nonlinear mathematical issues [13]. An input layer, one hidden layer, and output layer makes up the CNN structure that was taken into consideration for this study (**Figure 4**). Northings, Eastings, Elevations, Rock Quality Index (Q), Rock Quality Designation (RQD), Peak Particle Velocity, Internal Comprehensive Strength (ICS), Blast Distance, Log of Blast Distance, Density, and Displacement make up the 11 predictor variables that make up the input layer, according to the data used. Since the goal is to predict surface displacement, only one response variable is present in the output layer that is rate of displacement (ROD). **Figure 4** shows the network architecture of the CNN developed to achieve the optimum results for the prediction of surface displacement at the Monitoring Scan Point 3 (MSP3). By experimenting with different numbers of hidden neurons and choosing the ones that produced the greatest output results for each network architecture that was built, the uncertainty around the number of hidden neurons to be employed was removed. To increase prediction accuracy, the weights are periodically adjusted during CNN training by back-propagating the estimated error between the desired and predicted output [14] [15].

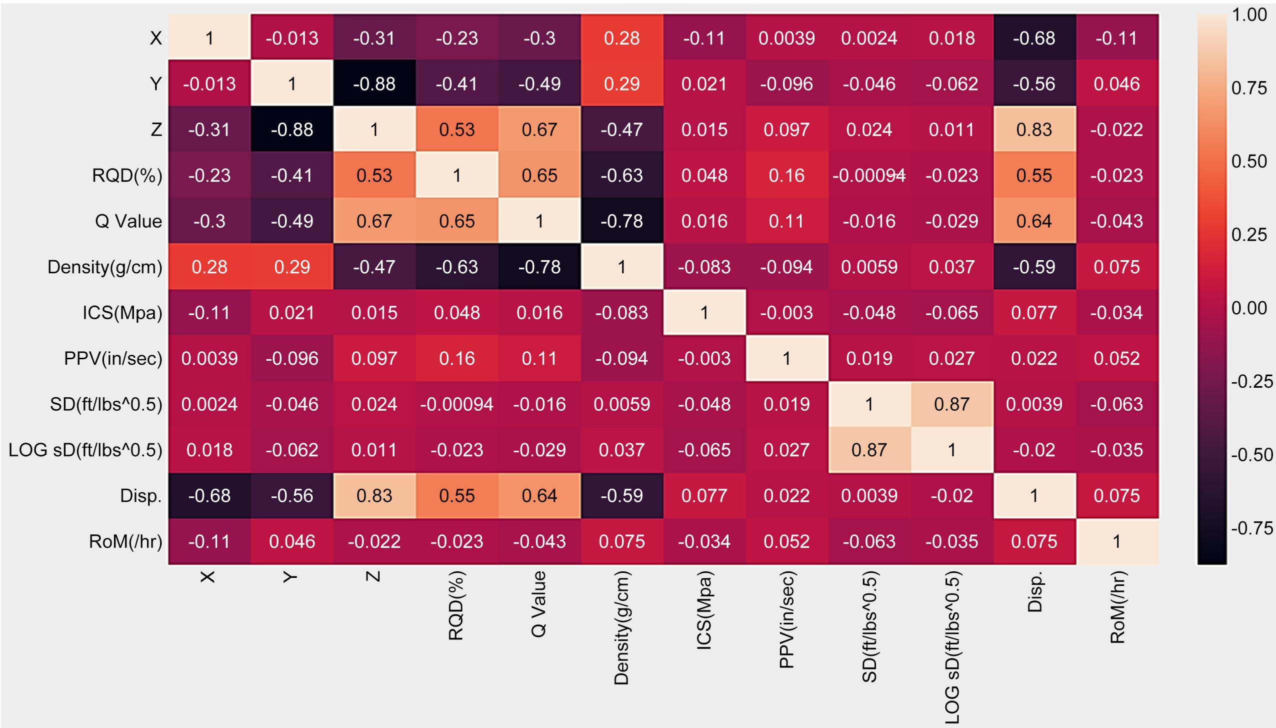

Figure 3. A correlation heatmap of displacement parameters.

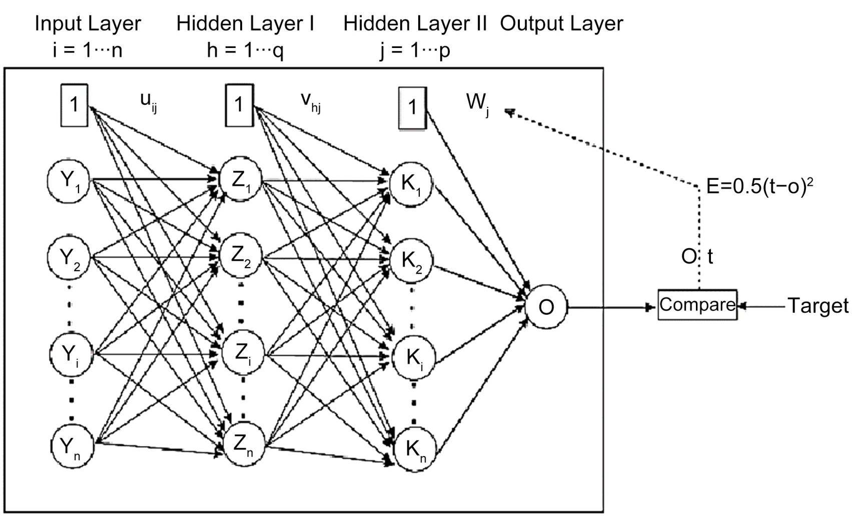

Figure 4. An architecture of convolutional neural network (Source: [13]).

2.3.3. Long Short-Term Memory (LSTM)

LSTM is used in this study, to learn, process, and classify sequential data. The core components of an LSTM network are a sequence of input layer and an LSTM layer. A sequence input layer inputs sequence or time steps of sequence data [16], [17]. The study considered 12 different readings for the Monitoring Scan Point 3 (MSP3) and among them are 11 inputs known as the predictor parameters which are Northings, Eastings, Elevations, Rock Quality Index (Q), Rock Quality Designation (RQD), Peak Particle Velocity, Internal Comprehensive Strength (ICS), Blast Distance, Log of Blast Distance, Density, and Displacement and an output known as Rate of Displacement (ROD). **Figure 5** and **Figure 6** show the LSTM process structure and architecture respectively.

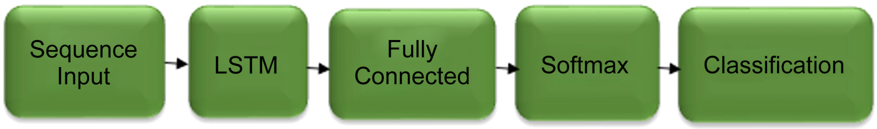

Figure 5. LSTM process structure.

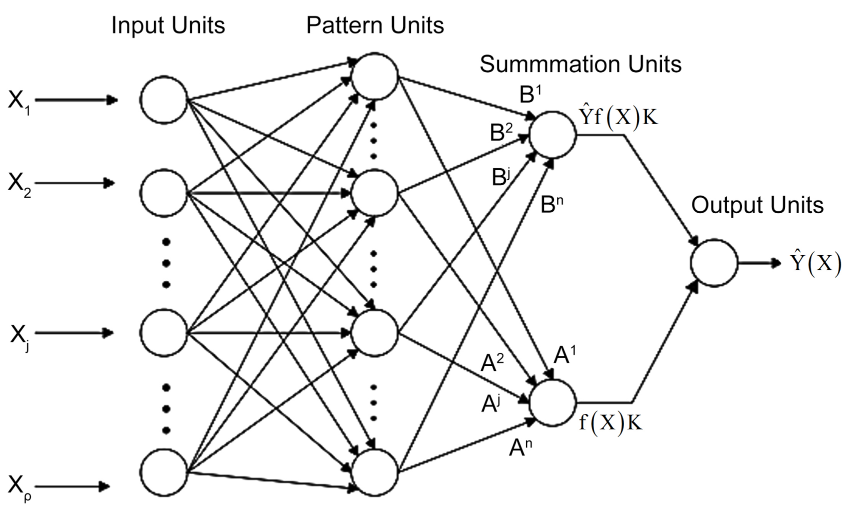

Figure 6. An architecture of long short-term memory (Source: [16]).

2.3.4. Hybrid Model

Studies have shown that combining two algorithms or more is more efficient than using only one approach in the AI domain, since these hybrid models exploit the strengths and overcome deficiencies of the individual algorithms [18]. The hybrid model as developed in this study comprises of two artificial neural network techniques for the prediction of surface displacement *i.e.*, CNN and LSTM. In the model, the 11 predictor variables were used and the Rate of Displacement (ROD) as the response variable. The data was divided into training and testing set with training set having 296 observations and testing set having 127 observations. The spatio-temporal dependency arises from different patterns [19] [20]. First, an LSTM model receives the input parameters to capture the dynamic temporal dependency occurring in the data, thus forming candidate feature data. A CNN model simultaneously captures the spatio-temporal dependency by performing convolutions on the candidate feature data, thus resulting in a spatio-temporal data (ST-Data). The final ST-data combines the external factors to obtain the prediction results. Finally, the model calculates the loss and optimises the parameters via back propagation. The following sections detail the main modules of C-LSTM. Figure 7 shows the framework of the proposed C-LSTM.

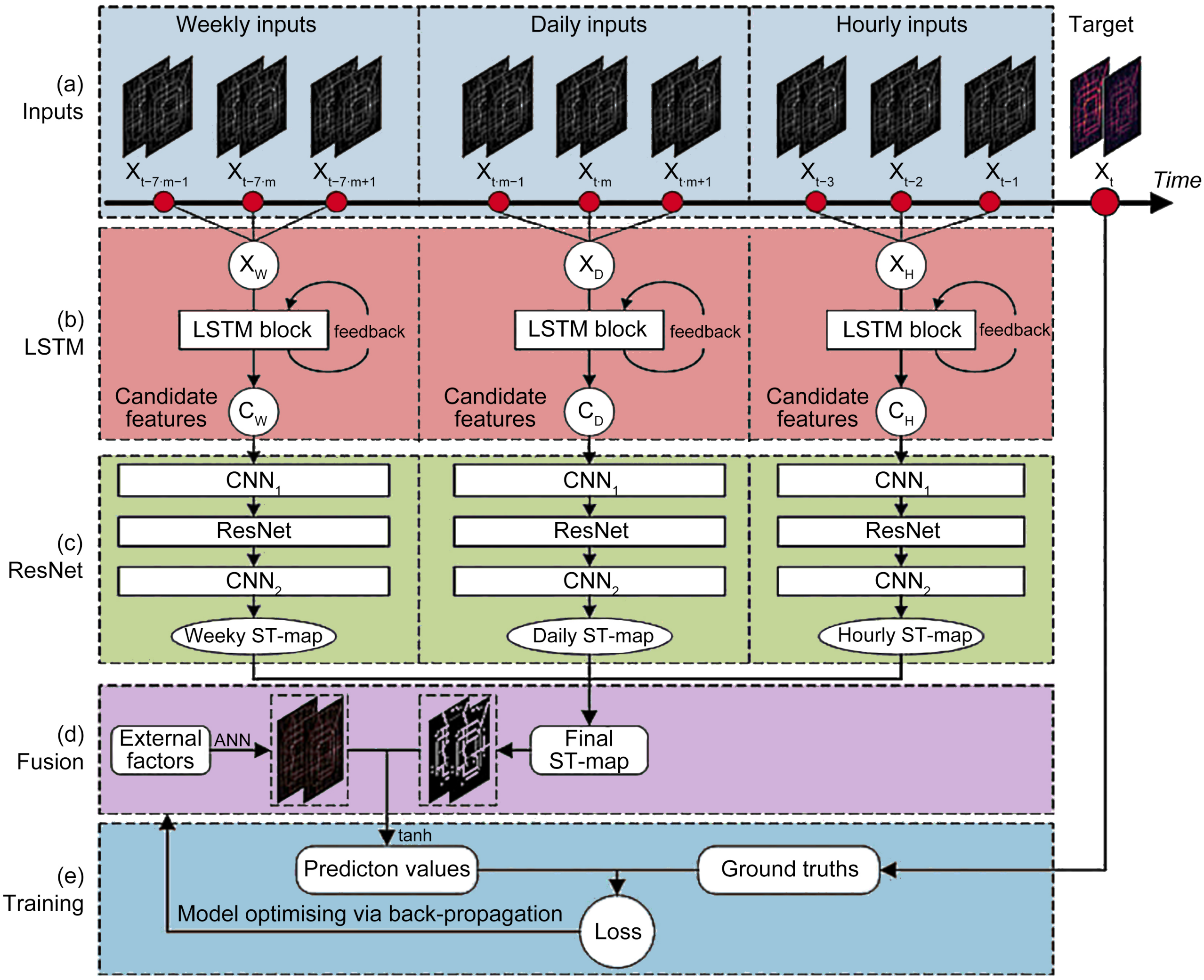

Figure 7. A flowchart of C-LSTM model (Source: [21]).

Input Datasets

The input datasets comprise of Northings, Eastings, Elevations, Rock Quality Index (Q), Rock Quality Designation (RQD), Peak Particle Velocity, Internal Comprehensive Strength (ICS), Blast Distance, Log of Blast Distance, Density, and Displacement. The northing, eastings and elevations are the geospatial location of the monitoring scan point 3 (MSP3), the density, peak particle velocity, rock quality index, rock quality designation, internal comprehensive strength index (ICS), and blast distance are the geotechnical parameters.

Integrally Capturing Spatio-Temporal Dependency

The core procedure of C-LSTM includes two components: capturing the temporal dependency using the LSTM (**Figure 7(b)**) and capturing the spatio-temporal dependency using CNN (**Figure 7(c)**).

2.3.5. Tuning Parameters

Parameter tuning is essential for identifying the optimal parameters for C-LSTM models [19] [21]. The hyper parameters are tuned to obtain the optimal prediction results of the C-LSTM model. There are four main hyper parameters: the number of hidden neuron units, number of hidden layers, lengths of different input patterns, and convolution kernel size. A number of hidden neuron units and number of hidden layers were integrated in this study.

Number of Hidden Neuron Units

The quantities denoted as FNLSTM and FNCNN correspond to the number of hidden units within the LSTM and CNN, respectively. When testing the LSTM, FNCNN is held constant at 64, while FNLSTM is systematically varied at values of four, eight, sixteen, and thirty-two. Similarly, in the case of testing the CNN, FNLSTM is maintained at 32, and FNCNN is adjusted across values of 4, 8, 16, 32, and 64. The LSTM architecture comprises two hidden layers, while the count of CNN units is incrementally raised from 1 to 13. The minimum RMSE is carefully recorded. The model attains its highest level of prediction accuracy, yielding an RMSE of 14.6, when FNLSTM is set to 32 and FNCNN is configured at 64.

Number of Hidden Layers

Two experiments were conducted to ascertain the ideal depth (number of hidden layers) for C-LSTM, focusing on evaluating the depths of LSTM (DLSTM) and CNN (DCNN) separately. The other parameters were held constant. In the first experiment, DLSTM was set at 2, while DCNN ranged from 1 to 13 in increments of two. Initially, the Root Mean Square Error (RMSE) exhibited a decline as DCNN increased, reaching its minimum value at DCNN equals 5, after which RMSE started to rise. The introduction of additional layers led to training challenges and noise, particularly at the displacement periphery. In the second experiment, focusing on LSTM, DCNN was set at 5, and DLSTM ranged from 1 to 4 with a step size of 1. The observed trend paralleled that of CNN, with the minimum RMSE achieved using two LSTM layers. Consequently, the optimal depths for HIDLST were determined to be two LSTM layers and five CNN units [22] [23].

2.3.6. Model Performance Evaluators

Identifying the most suitable model that effectively aligns with the data and produces the least predicted error is of utmost importance. The level of prediction error serves as a gauge of the model's performance, with lower error values signifying greater suitability for predictive tasks. Consequently, performance assessment metrics such as the Root Mean Square Error (RMSE) and Correlation Coefficient (R) were employed in this investigation. The mathematical expressions for these metrics are presented in Equations (1) and (2).

$$\text{RMSE} = \sqrt{\frac{\sum_{i=1}^{N}\left(Obs_i - Pred_i\right)^2}{N}} \tag{1}$$

$$R = \left(\frac{\sum_{i=1}^{N}\left(Obs_i - \overline{Obs_i}\right)\left(Pred_i - \overline{Pred_i}\right)}{\sqrt{\sum_{i=1}^{N}\left(Obs_i - \overline{Obs_i}\right)^2} \times \sqrt{\sum_{i=1}^{N}\left(Pred_i - \overline{Pred_i}\right)^2}}\right) \tag{2}$$

where; Obs_i and $Pred_i$ are the observed and predicted ROD, with $\overline{Obs}$ and $\overline{Pred}$, respectively, being their average corresponding values, and i range from 1 to N, where N denotes the entire amount of data.

3. Results and Discussion

The research utilised field datasets for training and evaluating the proposed surface displacement prediction model. Predicted results were subsequently compared with the outcomes of each individual prediction model. The inputs for each prediction model, as listed in **Table 1**, encompassed 11 parameters provided by the mining company. These inputs consisted of Northings, Eastings, Elevations, Rock Quality Index (Q), Rock Quality Designation (RQD), Peak Particle Velocity, Internal Comprehensive Strength (ICS), Blast Distance, Log of Blast Distance, Density, and Displacement. The model's output was the rate of displacement, which was determined through the use of a differential phase interferometric survey. To illustrate the rate of displacement against their respective timelines, **Figure 8** presents a line chart.

Table 1. A line chart of the rate of displacement.

Prediction Model	Input	Output
CNN LSTM C-LSTM	Eastings, Northings, Elevations, Peak Particle Velocity, Rock Quality Index, Rock Quality Designation, Internal Comprehensive Strength Index, and Blast Distance	Rate of Displacement

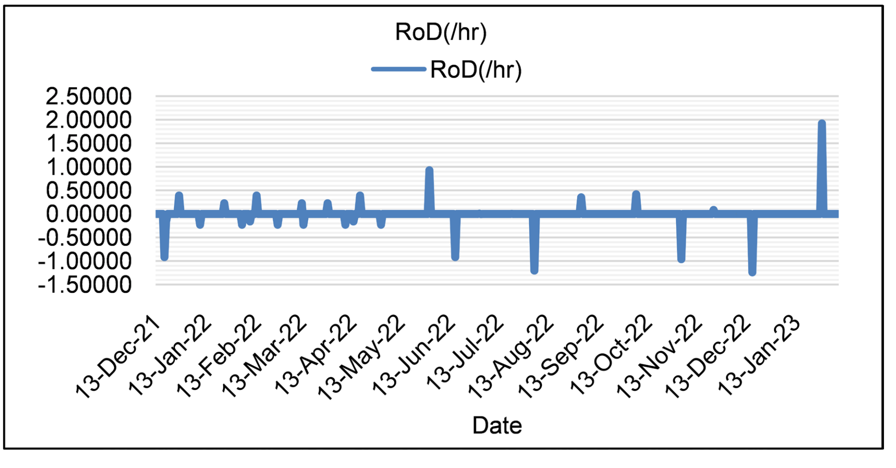

Figure 8. A line chart of the rate of displacement.

The model's practicability was evaluated using the testing data set. Below are the results of the developed predictive models.

3.1. Test Performance of the CNN Model

Surface displacement prediction for the Monitoring Scan Point 3 (MSP3) in the underground mine employed CNN. The challenge of determining the optimal number of hidden neurons was addressed through a sequential trial-and-error approach, involving the testing of various neuron quantities. The selection was based on the output results that exhibited the lowest RMSE, ultimately defining the optimal network structure. A matrix representation in **Table 2** summarises the application of various statistical evaluators to assess the validity of the developed CNN model. It is noteworthy that the CNN yielded notably low RMSE values for the MSP and achieved higher R values. The RMSE values approaching zero indicate a minimal differentiation between the CNN predictions and the observed displacement rate. This alignment is further supported by the dimensionless evaluators (R), illustrating a close-to-perfect association between the predicted and observed values. In **Figure 9**, a line chart displays the observed and predicted displacement rates over their respective timelines using the CNN.

Table 2. Performance assessment of the CNN model.

Performance/Data Partition	Testing	Training
RMSE (m)	0.08100	0.00505
R	0.98930	0.98410

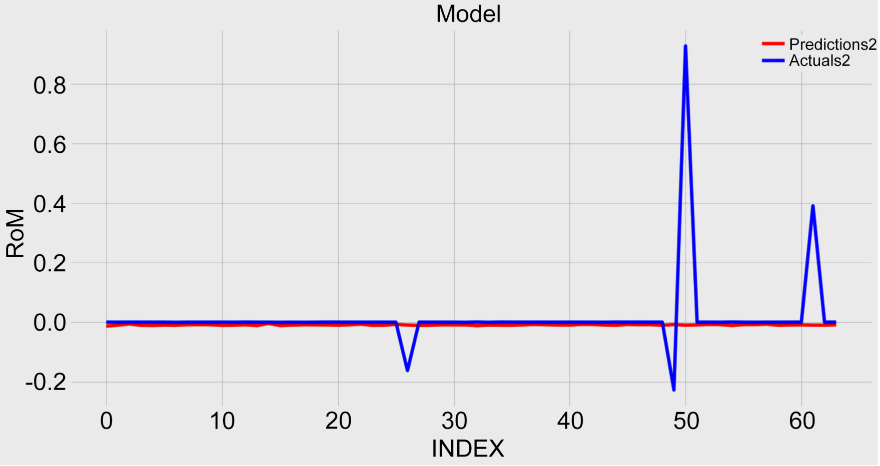

Figure 9. Line chart of actual and predicted rate of displacement using CNN.

3.2. Test Performance of the LSTM Model

Surface displacement prediction for the Monitoring Scan Point 3 (MSP3) in the underground mine involved the application of LSTM. The performance evaluation of the LSTM models is detailed in **Table 3**. The lower RMSE values and higher

R rates obtained suggest that the LSTM predictions align well with the observed displacement rate. Additionally, Figure 10 presents a line chart illustrating the observed and predicted displacement rates over their respective timelines using the LSTM.

Table 3. Performance assessment of the LSTM model.

Performance/Data Partition	Testing	Training
RMSE (m)	0.02370	0.00505
R	0.99951	0.99710

Figure 10. Line chart of actual and predicted rate of displacement using LSTM.

3.3. Test Performance of the C-LSTM Model

Subsequently, the primary focus of this study, C-LSTM, was applied to predict surface displacement for the Monitoring Scan Point 3 (MSP3) within the underground mine. Figure 11 illustrates a line chart depicting the observed and predicted displacement rates over their respective timelines using C-LSTM. A matrix representation of the C-LSTM model's efficiency for Monitoring Scan Point 3 (MSP3) in the underground mine is presented in Table 4. The minimal RMSE values obtained by C-LSTM for Monitoring Scan Point 3 (MSP3) indicate a nearly perfect fit to the observed data with minimal variation between the predicted and observed displacement rates. These findings are corroborated by C-LSTM achieving a high-accuracy R value. Hence, based on these results, C-LSTM emerges as the superior and exemplary model for forecasting surface displacement.

Table 4. Performance assessment of the C-LSTM model.

Performance/Data Partition	Testing	Training
RMSE (m)	0.02625	0.00306
R	0.99981	0.99918

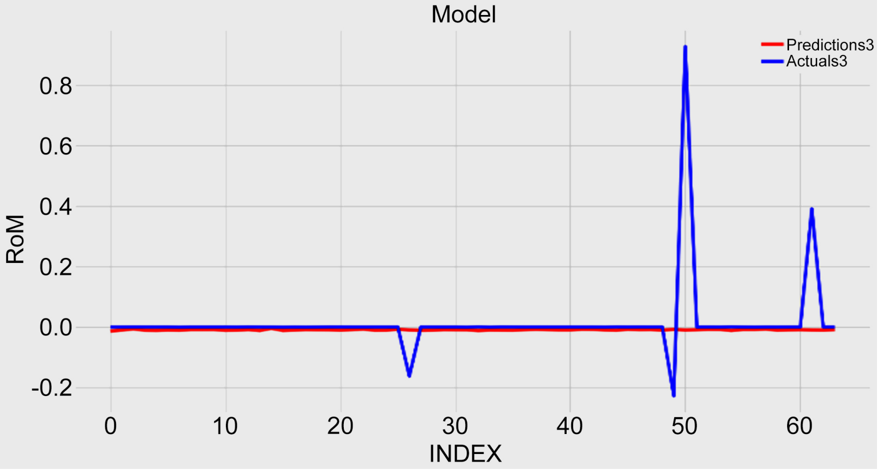

Figure 11. Line chart of actual and predicted rate of displacement using C-LSTM.

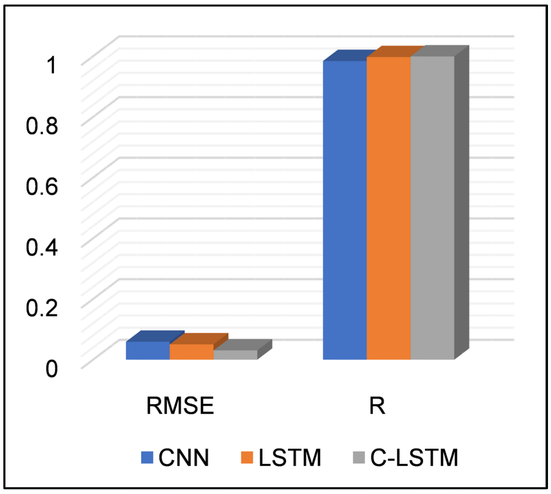

Figure 12. A bar chart of the RMSE and R of the training dataset of all the models.

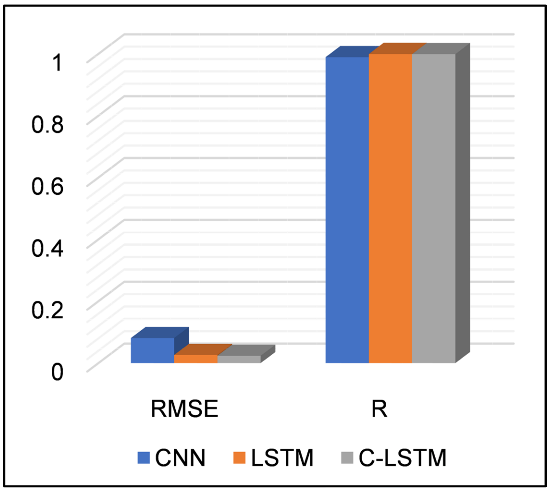

Figure 13. A bar chart of the RMSE and R of the testing dataset of all the models.

3.4. Comparing the Three Models Performance

Figure 12 and Figure 13 show bar charts of RMSE and R of the training and testing respectively, for all the models developed. All the models predicted unique and excellent results, but based on the results in Table 2, Table 3 and Table 4, the C-LSTM provided the most excellent results.

4. Conclusions and Recommendations

In conclusion, an evaluation of the C-LSTM hybrid model for surface displacement prediction has been undertaken. The model is based on integrating two artificial neural network models, LSTM and CNN to form C-LSTM. The capacity of this hybrid model to capture dynamic temporal dependencies within input characteristics provides a substantial advantage over individual prediction models. In summary, the spatial and dynamic temporal dependencies in surface displacement data from underground mines can be automatically and accurately captured by C-LSTM. The model's performance has been assessed using RMSE and R, revealing exceptional performance. The experimental results demonstrate that the C-LSTM model surpasses the performance of the separate models, LSTM and CNN. In light of the results and conclusions presented, it is recommended that the developed hybrid model be adopted by mining companies for surface displacement prediction in underground mines to enhance safety operations. An accurate prediction of surface displacement can facilitate effective planning for addressing various surface displacement scenarios. Furthermore, it is suggested that additional hybrid artificial intelligence models be developed and compared with the C-LSTM model to further assess their efficiency and superiority. These models may encompass the utilisation of the Particle Swarm Optimisation (PSO) algorithm in conjunction with artificial neural networks, such as the Gorilla Troop Optimisation Algorithm and LSTM (GTO-LSTM).

Acknowledgements

The authors wish to thank management of the University of Mines and Technology (UMaT), and the Department of Geomatic Engineering for using their state-of-art GIS laboratory to process and analyse data for this research.

Conflicts of Interest

The authors declare no conflicts of interest regarding the publication of this paper.

References

[1] Faramarzi, F., Farahmand, N. and Mozaffari, M. (2016) A Comparison between Artificial Neural Networks and Multiple Regression Analysis to Predict Ground Vibration Produced by Bench Blasting. *Engineering Science and Technology Journal*, **19**, 33-40.

[2] Bell, A.S. and Sadler, I.H. (2002) A Review of Ground Fall Accidents in UK Mines. *Safety Science*, **40**, 623-641.

[3] Aydin, C. (2011) Geodetic Deformation Analysis. Unpublished BSc Lecture Notes, Yildiz Technical University, Istanbul, 1-13.

[4] Beshr, A.A.E.W. (2015) Structural Deformation Monitoring and Analysis of Highway Bridge Using Accurate Geodetic Techniques. *Engineering*, **262**, 214-222.

[5] Kumar, R., Choudhury, D. and Bhargava, K. (2016) Simulation of Rock Subjected to Underground Blast Using FLAC3D. *Japanese Geotechnical Society Special Publication*, **2**, 508-511. https://doi.org/10.3208/jgssp.ind-27

[6] Khandelwal, M., Singh, T.N. and Shrivastava, P. (2017) Support Vector Machine and Artificial Neural Network Models for Prediction of Rock Mass Modulus. *Neural Computing and Applications*, **28**, 311-314.

[7] Singh, R.P. and Yadav, R.N. (1995) Prediction of Subsidence Due to Coal Mining in Raniganj Coalfield, West Bengal, India. *Engineering Geology*, **39**, 103-111. https://doi.org/10.1016/0013-7952(94)00062-7

[8] Suryanita, R., Jingga, H. and Yuniarto, E. (2016) The Application of Artificial Neural Networks in Predicting Structural Response of Multistory Building in the Region of Sumatra Island. *Conference of Science and Engineering for Instrumentation, Environment and Renewable Energy*, Pekanbaru, 28-29 September 2015, 71. https://doi.org/10.18502/keg.v1i1.526

[9] Chern, S., Tsai, J.H., Chien, L.K. and Huang, C.Y. (2009) Predicting Lateral Wall Deflection in Top-Down Excavation by Neural Network. *International Journal of Offshore and Polar Engineering*, **19**, 151-157.

[10] Zhang, W., Zhang, Y. and Goh, A.T.C. (2017) Multivariate Adaptive Regression Splines for Inverse Analysis of Soil and Wall Properties in Braced Excavation. *Tunnelling and Underground Space Technology*, **64**, 24-33. https://doi.org/10.1016/j.tust.2017.01.009

[11] Wang, J., Cheng, T. and Li, X. (2007) Nonlinear Integration of Spatial and Temporal Forecasting by Support Vector Machines. *Fourth International Conference on Fuzzy Systems and Knowledge Discovery* (*FSKD* 2007), Haikou, 24-27 August 2007, 61-66. https://doi.org/10.1109/fskd.2007.424

[12] Kaplan, M.O., Ayan, T. and Erol, S. (2004) The Effects of Geodetic Configuration of the Network in Deformation Analysis. *FIG Working Week* 2004, Athens, 22-27 May 2004, 55-70.

[13] Rumelhart, D.E., Hinton, G.E. and Williams, R.J. (1986) Learning Representations by Back-Propagating Errors. *Nature*, **323**, 533-536. https://doi.org/10.1038/323533a0

[14] Macloed, C. (2020) An Introduction to Practical Neural Networks and Genetic Algorithms for Engineers and Scientists. Ph.D. Thesis, The Robert Gordon University.

[15] Simonyan, K. and Zisserman, A. (2014) Very Deep Convolutional Networks for Large-scale Image Recognition. arXiv: 1409.1556. https://doi.org/10.48550/arXiv.1409.1556

[16] Wu, H., Dong, Y., Shi, W., Clarke, K.C., Miao, Z., Zhang, J., *et al.* (2015) An Improved Fractal Prediction Model for Forecasting Mine Slope Deformation Using GM (1, 1). *Structural Health Monitoring*, **14**, 502-512. https://doi.org/10.1177/1475921715599050

[17] Ma, X., Tao, Z., Wang, Y., Yu, H. and Wang, Y. (2015) Long Short-Term Memory Neural Network for Traffic Speed Prediction Using Remote Microwave Sensor Data. *Transportation Research Part C: Emerging Technologies*, **54**, 187-197. https://doi.org/10.1016/j.trc.2015.03.014

[18] Bacanin, N., Zivkovic, M., Al-Turjman, F., Venkatachalam, K., Trojovský, P., Strumberger, I., *et al.* (2022) Hybridized Sine Cosine Algorithm with Convolutional Neural Networks Dropout Regularization Application. *Scientific Reports*, **12**, Article No. 6302. https://doi.org/10.1038/s41598-022-09744-2

[19] Zhang, C., Li, J.-Z. and He, Y. (2019) Application of Optimized Grey Discrete

Verhulst-BP Neural Network Model in Settlement Prediction of Foundation Pit. *Environmental Earth Sciences*, **78**, Article No. 441. https://doi.org/10.1007/s12665-019-8458-y

[20] He, X.P., Hua, X.S. and He, X.F. (2007) Weighted Multi-Point Grey Model and Its Application to High Rock Slope Deformation Forecast. *Rock and Soil Mechanics*, **6**, 1187-1191.

[21] Ke, J., Zheng, H., Yang, H. and Chen, X. (2017) Short-Term Forecasting of Passenger Demand under on-Demand Ride Services: A Spatio-Temporal Deep Learning Approach. *Transportation Research Part C: Emerging Technologies*, **85**, 591-608. https://doi.org/10.1016/j.trc.2017.10.016

[22] He, H. (2017) Multifractal Analysis of Interactive Patterns between Meteorological Factors and Pollutants in Urban and Rural Areas. *Atmospheric Environment*, **149**, 47-54. https://doi.org/10.1016/j.atmosenv.2016.11.004

[23] He, K., Zhang, X., Ren, S. and Sun, J. (2016) Deep Residual Learning for Image Recognition. 2016 *IEEE Conference on Computer Vision and Pattern Recognition* (*CVPR*), Las Vegas, 27-30 June 2016, 770-778. https://doi.org/10.1109/cvpr.2016.90